

Electronic Supporting Information

Surface Design of Core-Shell Superparamagnetic Iron Oxide Nanoparticles Drives Record Relaxivity Values in Functional MRI Contrast Agents

Dipak Maity, Giorgio Zoppellaro, Veronika Sedenkova, Jiri Tucek, Klara Safarova, Katerina Polakova, Katerina Tomankova, Clemens Diwocky, Rudolf Stollberger, Libor Machala, and Radek Zboril

Contents

Chemicals	pg.3
Synthesis of ATA-SPIO	pg.3
Synthesis of TA-SPIO	pg.4
Instrumental Techniques and Characterization Methods	pg.5
Figure S1: Aqueous suspension of TA-SPIO and ATA-SPIO nanoparticles.	pg.8
Figure S2: XRD patterns ATA-SPIO and TA-SPIO.	pg.8
Figure S3: TEM images of TA-SPIO.	pg.9
Figure S4: SEM images and EDS analyses of ATA-SPIO and TA-SPIO.	pg.9
Figure S5: FT-IR spectra of ATA-SPIO and TA-SPIO.	pg.10
Figure S6: TGA analysis ATA-SPIO and TA-SPIO.	pg.10
Figure S7: DLS measurements of ATA-SPIO ferrofluid suspension in DI water (pH = 7) after 24 h of storage in dark at room temperature.	pg.11
Figure S8: The zeta-potential of ATA-SPIO ferrofluid suspension in DI water (pH = 7) after 24 h of storage in dark at room temperature.	pg.12
Figure S9: DLS measurements of ATA-SPIO ferrofluid suspension in DI water (pH = 7) after more than 3 months of storage in dark at 4 °C.	pg.13
Figure S10: DLS measurements of TA-SPIO ferrofluid suspension in DI water (pH = 7) after 24 h of storage in dark at room temperature.	pg.14
Figure S11: The zeta-potential of TA-SPIO ferrofluid suspension in DI water (pH = 7) after 24 h of storage in dark at room temperature.	pg.15
Figure S12: DLS measurements of TA-SPIO ferrofluid suspension in DI water (pH = 7) after more than 3 months of storage in dark at 4 °C.	pg.16
Figure S13: DLS measurements of ATA-SPIO ferrofluid suspension in physiological salt solution (pH = 7, 150 mM of NaCl) after 1 day of storage in dark at room temperature.	pg.17
Figure S14: DLS measurements of ATA-SPIO ferrofluid suspension in physiological salt solution (pH = 7, 150 mM of NaCl) after 1 day of storage in dark at room temperature.	pg.18

Figure S15: Plots for r_1 , r_2 and r_2^* of ATA-SPIO nanoparticles.	pg.19
Figure S16: Plots for r_1 , r_2 and r_2^* of TA-SPIO nanoparticles.	pg.20
Figure S17: Negative of the phantom experiments of TA-SPIO and ATA-SPIO.	pg.21
Figure S18: Correlation between SPIO surface design and ATA-SPIO and TA-SPIO MRI negative contrast performances.	pg.22
Table S1: Bulk susceptibility analyses of ATA-SPIO and TA-SPIO.	pg.23
Table S2: Mössbauer hyperfine parameters of ATA-SPIO and TA-SPIO.	pg.24
Table S3: Relaxivity indexes r_1 , r_2 and r_2^* of ATA-SPIO and TA-SPIO nanoparticles.	pg.25

Chemicals

Analytical grade ferric chloride ($\text{FeCl}_3 \times 6 \text{H}_2\text{O}$), ferrous chloride ($\text{FeCl}_2 \times 4 \text{H}_2\text{O}$), 2-aminoterephthalic acid (ATA, $\text{C}_8\text{H}_7\text{NO}_4$), terephthalic acid (TA, $\text{C}_8\text{H}_6\text{O}_4$), ammonium hydroxide (NH_4OH , 29%) were used.

Synthetic Preparation of ATA/TA-SPIO hybrid systems

Synthesis of ATA-SPIO

Reagents:

(A) 2.34 g $\text{FeCl}_3 \times 6 \text{H}_2\text{O}$ (ACS reagent, 97% purity, MW = 270.30 g/mol, CAS: 10025-77-1)

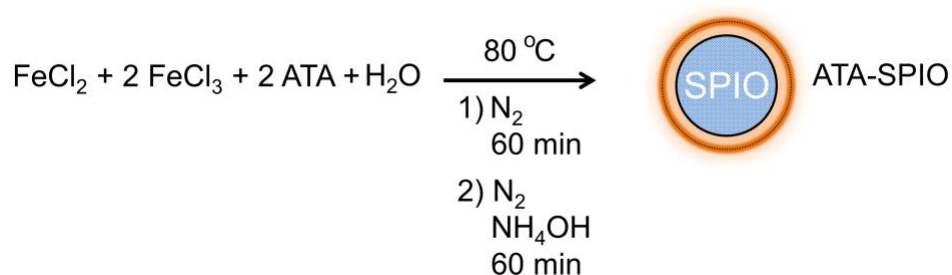
(B) 0.86 g $\text{FeCl}_2 \times 4 \text{H}_2\text{O}$ (> 99.0% purity, MW = 198.81, CAS: 13478-10-9)

(C) 1.65 g of ATA (2-amino-terephthalic acid, MW = 181.15 g/mol, CAS: 10312-55-7)

(D) 45 mL of deionized (DI) water

(E) 5 mL of NH_4OH

Reagents (A) to (D) were added in a reaction vessel together, heated at 80°C for 1 h (60 min) under magnetic stirring (400 rpm), with nitrogen gas flow directly blowing in the reaction vessel. Then (E) (NH_4OH , 29% in water, 14.8 M, $\rho = 0.90 \text{ g/mL}$, CAS: 1336-21-6) was added rapidly into the solution, which resulted in nucleation of SPIO particles. The resulting suspension was kept at 80°C for another 1 h (60 min) under vigorous magnetic stirring (1000 rpm) and then cooled down to room temperature. The final pH of the solution was $10.0 < \text{pH} < 11.0$. The so-formed black magnetic nanoparticles were magnetically isolated and washed with mixture of DI water and ethanol (10 mL, 1:1 vol/vol) several times (4 washings) allowing isolation of 3.25 g of coated ATA-SPIO. Upon using twice amounts of reagents (A) to (E), twice amount (6.50 g) of ATA-SPIO particles were obtained. The particles dispersed in DI water gave stable aqueous ferrofluid suspensions (weeks), the particles dried overnight in oven did not show surface degradation after weeks of storage under air.



Synthesis of TA-SPIO

Reagents:

(A) 2.34 g $\text{FeCl}_3 \times 6 \text{H}_2\text{O}$ (ACS reagent, 97% purity, MW = 270.30 g/mol, CAS: 10025-77-1)

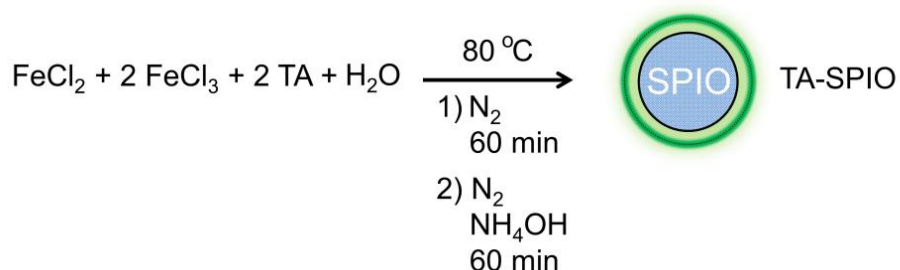
(B) 0.86 g $\text{FeCl}_2 \times 4 \text{H}_2\text{O}$ (> 99.0% purity, MW = 198.81, CAS: 13478-10-9)

(C) 1.51 g of TA (terephthalic acid, MW = 166.13 g/mol, CAS: 100-21-0)

(D) 45 mL of deionized (DI) water

(E) 5 mL of NH_4OH

Reagents (A) to (D) were added in a reaction vessel together, heated at 80°C for 1 h (60 min) under magnetic stirring (400 rpm), with nitrogen gas flow directly blowing in the reaction vessel. Then (E) (NH_4OH , 29% in water, 14.8 M, $\rho = 0.90 \text{ g/mL}$, CAS: 1336-21-6) was added rapidly into the solution, which resulted in nucleation of SPIO particles. The resulting suspension was kept at 80°C for another 1 h (60 min) under vigorous magnetic stirring (1000 rpm) and then cooled down to room temperature. The final pH of the solution was $10.0 < \text{pH} < 11.0$. The so-formed black magnetic nanoparticles were magnetically isolated and washed with mixture of DI water and ethanol (10 mL, 1:1 vol/vol) several times (4 washings) allowing isolation of 3.15 g of coated TA-SPIO. Upon using twice amounts of reagents (A) to (E), twice amount (6.30 g) of TA-SPIO particles were obtained. The particles dispersed in DI water gave stable aqueous ferrofluid suspensions (weeks), the particles dried overnight in oven did not show surface degradation after weeks of storage under air.



Instrumental Techniques and Characterization Methods

Scanning electron microscope (SEM) micrographs and energy-dispersive spectroscopy (EDS) were taken on a Hitachi 6600 FEG microscope. Dried powder samples were placed on aluminum holder with double-sided adhesive carbon tape. The accelerating voltage of 5 keV was used.

Transmission electron microscope (TEM) micrographs and selected area electron diffractions (SAED) were taken on a JEOL 2010 microscope operating at 200kV with a point-to-point resolution of 1.9 Å. Before measurements, aqueous ferrofluid suspension was much diluted with DI water, and treated in ultrasound for 5 minutes. A drop of the dilute suspension was placed onto a holey-carbon film supported by a copper-mesh TEM grid and air-dried at room temperature.

Particle size distribution of SPIO nanoparticles were determined by dynamic light scattering (DLS) instrument (Zetasizer, MALVERN, UK). The samples were prepared from stock NPs solutions (in DI) by diluting the ferrofluid suspensions with DI water or 0.15 M NaCl solution at an optimum concentration of particles, procedure necessary for getting accurate measurement by DLS, and further treated in ultrasound water-bath for few minutes. About 2-3 mL of the samples was taken in the cuvette. Then the cuvette was placed inside the cavity of DLS instrument and particle sizes and size distributions were measured by DLS Nano-ZS software as well as zeta-potential. Stock solutions were made as follows: **(a)** 59 mg of dried ATA-SPIO NPs were suspended in 1 mL of DI water and sonicated for 5 min. The final concentration of the ferrofluid suspension of nanoparticles was 59×10^3 ppm, and the [Fe] was 42×10^3 ppm. **(b)** 57 mg of dried TA-SPIO were suspended in 1 mL of DI water and sonicated for 5 min. The final concentration of the ferrofluid suspension of nanoparticles was 57×10^3 ppm, and the [Fe] was 40.6×10^3 ppm. The stock solutions were kept under dark at 4 °C, unless otherwise stated. The dilution employed of the stock solutions for the DLS experiments were obtained as follow: 200 µL of stock-solution + 99.8 mL of solvent (DI water or 0.15 M NaCl solution, pH = 7) were mixed together and sonicated for 3 minutes at room temperature (new concentration of **(c)** ATA-SPIO NPs = 118 ppm and new concentration of **(d)** TA-SPIO NPs = 114 ppm). Then, 1 mL of suspension **(c)** of ATA-SPIO NPs or 1 mL of suspension **(d)** of TA-SPIO NPs were mixed with 2 mL of DI water or 2 mL of 0.15 M NaCl solution, in order to obtain the final suspensions used for DLS experiments of **(e)** ATA-SPIO (NPs ~39 ppm) and **(f)** ATA-SPIO (NPs = 38 ppm), which were stored in dark. We did notice that very concentrated (e.g. stock solutions **a** and **b**) and diluted solutions of NPs (e.g. solutions **e** and **f**) were very stable, showing no hint of precipitation after several weeks, while the intermediate concentration (namely **c** and **d**) showed hint of some nanoparticle's precipitation after 2 days, both at room temperature and when stored in cold (4 °C).

X-ray powder diffraction (XRD) patterns of all solid samples were recorded on X'Pert PRO (PANalytical, The Netherlands) instrument in Bragg–Brentano geometry with iron-filtered CoK α radiation (40 kV, 30 mA, λ = 0.1788965 nm) equipped with an X'Celerator detector and programmable divergence and diffracted beam antiscatter slits.

Atomic absorption. The total content of iron present in the samples was determined by atomic absorption spectroscopy (AAS) with flame ionization using Perkin Elmer 3300 device (Perkin Elmer, USA).

Mössbauer spectroscopy. The transmission ^{57}Fe Mössbauer spectra were measured using a Mössbauer spectrometer in a constant acceleration mode with a $^{57}\text{Co}(\text{Rh})$ source. The isomer shift values were related to $\alpha\text{-Fe}$ at room temperature. The measurements were carried out in a closed-helium cycle device at a temperature of 300 and 150 K without the application of an external magnetic field. The samples for Mössbauer spectroscopy were prepared with a great care concerning the constant amount and thickness. The acquired Mössbauer spectra were fitted with the MossWinn software package; prior to fitting, the signal-to-noise ratio was enhanced by a statistically based algorithm developed by Prochazka et al.¹

(1) Prochazka, R.; Tucek, P.; Tucek, J.; Marek, J.; Mashlan, M.; Pechousek, J. *Meas. Sci. Technol.* 2010, **21**, 025107.

Bulk magnetic susceptibility. A superconducting quantum interference device (SQUID, MPMS XL-7, Quantum Design, USA) was employed for the bulk magnetic measurements. The hysteresis loops were collected at a temperature of 5 and 300 K in external magnetic fields ranging from -70 to $+70$ kOe. The zero-field-cooled (ZFC) and field-cooled (FC) magnetization curves were recorded on warming in the temperature range from 5 to 300 K and in an external magnetic field of 1 kOe after cooling in a zero magnetic field and a field of 1 kOe, respectively.

Fourier transform infrared (FT-IR) spectra of the dried samples were recorded on a Nexus 670 FTIR spectrometer (Thermo Nicolet) using a Smart Orbit diamond ATR technique ($400\text{--}3600\text{ cm}^{-1}$).

Thermogravimetric analyses (TGA) were carried out on a Thermal Analyser Exstar (TG/DTA 6200, Seiko Instruments Inc.) taking 15-20 mg samples in a platinum crucible under flowing nitrogen ($70\text{ cm}^3\text{ min}^{-1}$) with the heating rate of $5\text{ }^\circ\text{C min}^{-1}$ from room temperature to 800°C .

In vitro biocompatibilities of the nanoparticles (NPs) were evaluated by cytotoxicity studies on NIH3T3 cells (mouse fibroblast cells) was determined using the MTT assay. During impact of NPs in concentrations 500, 250, 125, 60, 30, 15, 7 and $0\text{ }\mu\text{g/mL}$ cells were incubated in 96 well plates (P-Lab, Czech Republic) at $37\text{ }^\circ\text{C}$ and 5 % CO_2 for 24 h. Before starting the MTT experiments we replaced DMEM (Dulbecco's Modified Eagle Medium with 10% Fetal Bovine Serum) by PBS (phosphate buffered saline, $\text{pH} = 7.4$), containing 5 mM glucose, added $10\text{ }\mu\text{L}$ 20 mM MTT (3-(4,5-dimethyl-2-thiazolyl)-2,5-diphenyl-2H-tetrazolium bromide) dissolved in PBS and incubated the cells for 3 h at $37\text{ }^\circ\text{C}$ and 5 % CO_2 . The MTT solution was carefully removed and $100\text{ }\mu\text{L}$ DMSO we added in order to solubilize the violet formazan crystals. The absorbance of the resulting solution was measured in 96-well microplate reader Synergy HT (BioTek, USA) at 570 nm. The cell viability of the samples was determined as percentage of control cell viability ($100 \times \text{average of test group}/\text{average of control group}$). IC_{50} was statistically determined by 3T3NRU Phototox software (COLIPA, Germany).

Magnetic Resonance Imaging (MRI) and Relaxometry measurements were performed with a clinical 3T whole-body MR scanner (Siemens Skyra, Erlangen, Germany). For all measurements an 8-channel multipurpose array coil (Noras 8Ch CPC, Höchberg, Germany) was used to gain high Signal-to-Noise ratio. Aqueous ferrofluid suspension was diluted with H₂O bidest and mixed with 1% agarose 1:1. A dilution series starting from 0.5 mM Fe to 0.031 mM was filled into cylindrical cavities within a solidified 1% agarose gel in order to avoid susceptibility induced B₀ inhomogeneities caused by air/agar interfaces. R₂ relaxometry measurements were realized with a 2D Carr-Purcell-Meiboom-Gill (CPMG) sequence with an echo-spacing of 11.1ms and 24 echos, TR = 5000 ms, FOV = 90 × 73 mm, phase-oversampling(OS) = 50%, matrix = 192 × 156 and a single 5 mm slice. R₂* was determined using a 2D Multi-Echo-Gradient-Echo (GRE) sequence with 12 echo times ranging from 2.69 ms to 22.82 ms, TR = 500 ms, alpha = 25°, NEX = 4, FOV = 90 × 70mm, phase-OS = 60%, matrix = 100 × 128 and a single 5 mm slice. In addition, a T₂* weighted image was taken at TE=19ms. R₁ was measured employing an Inversion-Recovery-Fast-Spin-Echo (IR-FSE) and 6 different inversion times (50, 100, 200, 400, 800, 1600, 3200 ms), at a temperature of 23.2 °C, a turbo-factor of 3, TR = 5000 ms, FOV = 90 × 73 mm, phase-OS = 50%, matrix = 192 × 156 and a single 5 mm slice. T₂ weighted image was taken at TE = 99 ms. Transverse and Longitudinal (T_L) relaxation times were calculated using a self-written program (IDL, Exelis Inc., CO, USA). T₂ and T₂* were determined with a linear fit of the logarithm signal intensity over echo time (for all used TEs the SNR was > 5) whereas for the CPMG sequence the first echo was ignored. T₁ was calculated using a 3-parameter fit of the IR-FSE dataset according to the signal equation

$$S_{\text{IR}} = A \times [1 - B \exp(-T_1/T_L)].$$

Finally, r_1 , r_2 and r_2^* were computed as the slope of the linear regression between R₁, R₂, and R₂* and Fe concentration in mM.

Supporting Figures

Figure S1: (a) Aqueous suspension of TA-SPIO nanoparticles (ferrofluid) immediately after preparation, and (b) aqueous ferrofluid suspension of ATA-SPIO exposed to an external magnet with concentration of $N_p = 120$ mg/mL.

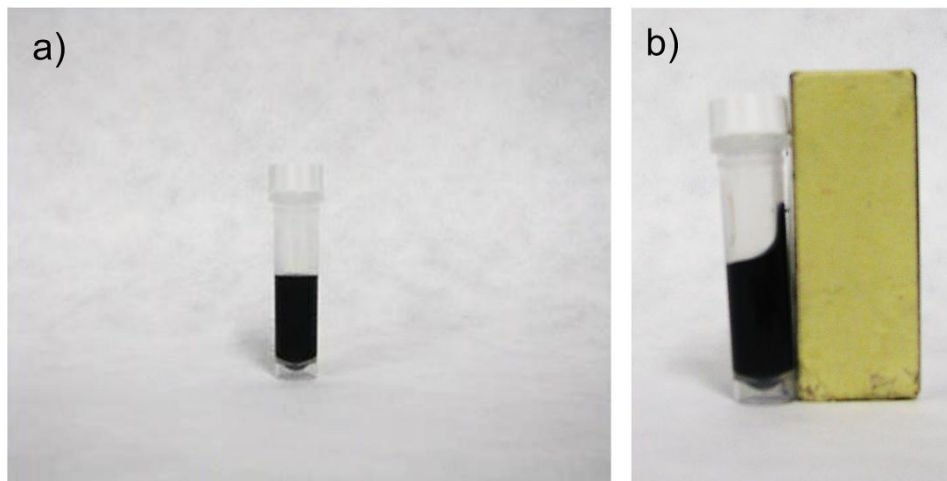


Figure S2: XRD patterns of (black-line) ATA-SPIO and (red-line) TA-SPIO.

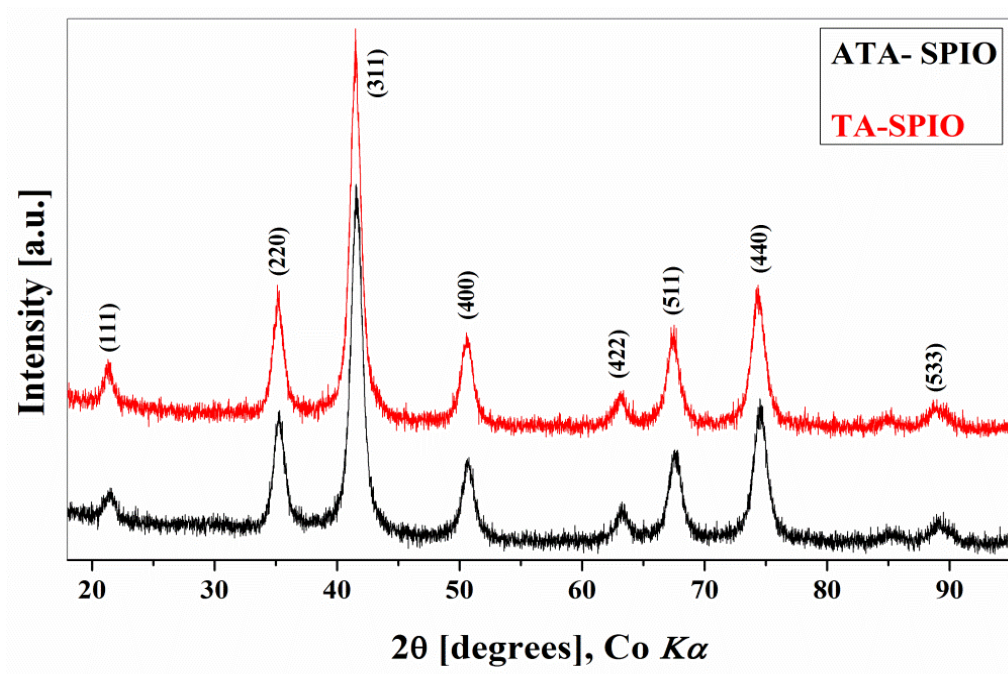


Figure S3: TEM images of TA-SPIO NPs. In panel (b) the arrow highlights crystalline planes. Size bars 100 nm in (a) and 20 nm in (b).

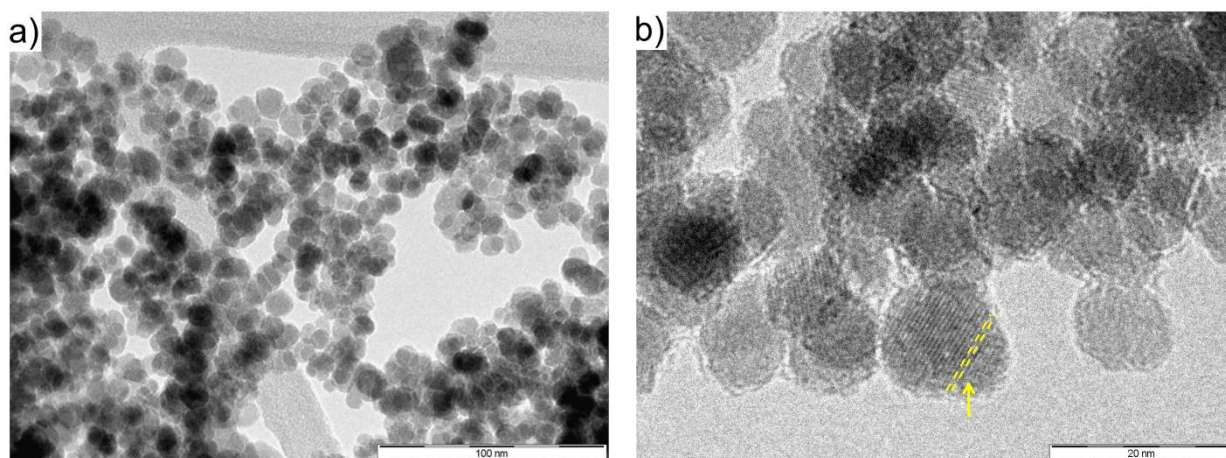


Figure S4: SEM image of dried-powder of (a) ATA-SPIO and (c) TA-SPIO. The Energy Dispersive Spectrometry (SEM-EDS) pattern for ATA-SPIO is shown in Panel (b) and for TA-SPIO in Panel (d).

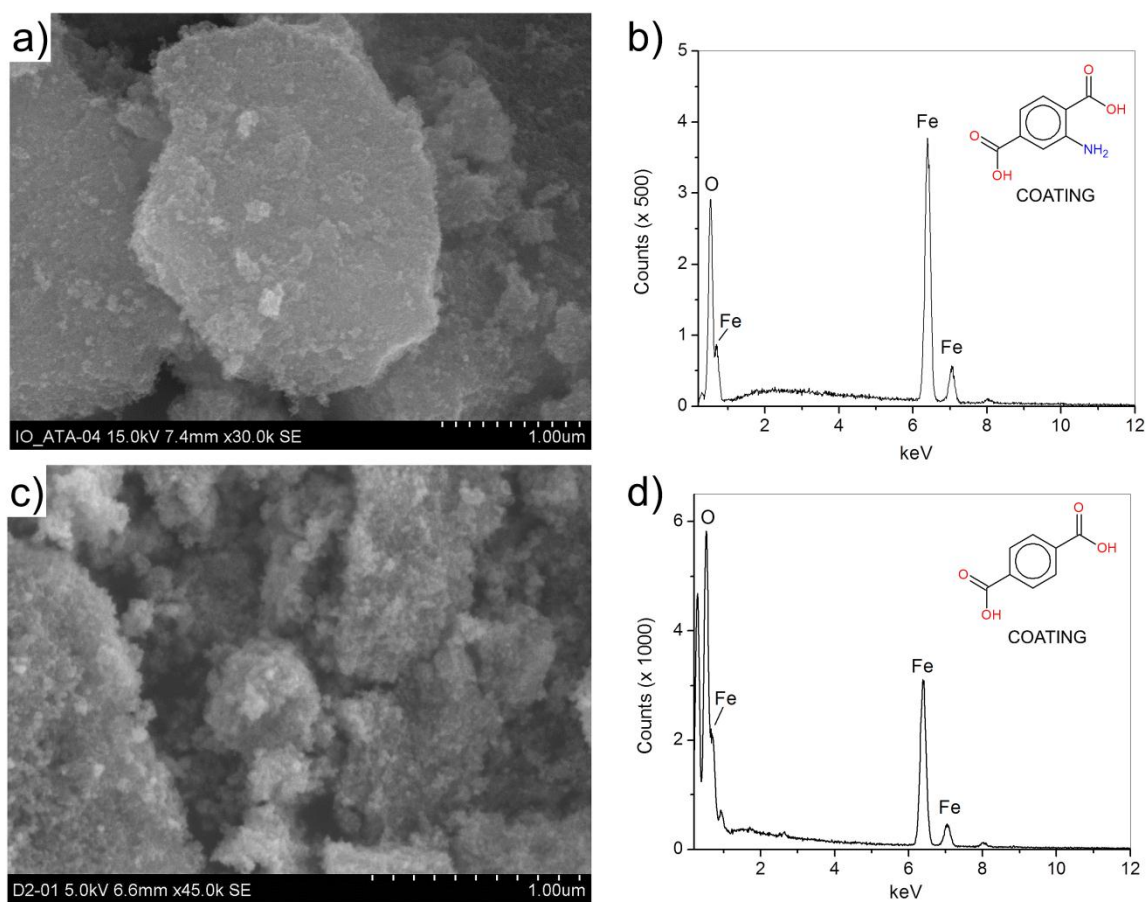


Figure S5: FT-IR spectra of (black-line) ATA-SPIO and (red-line) TA-SPIO.

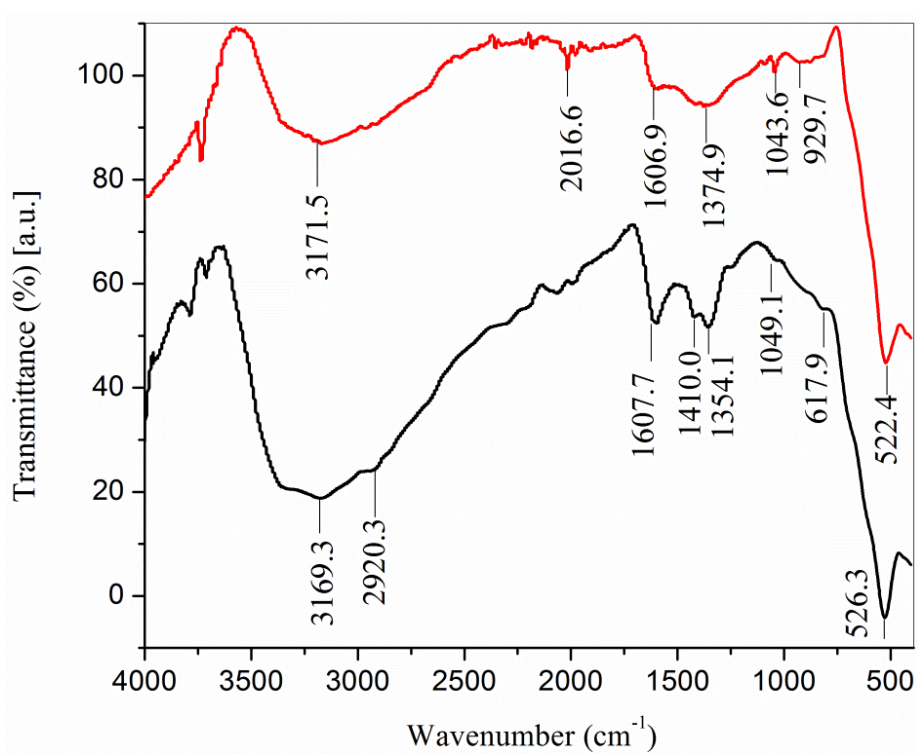


Figure S6: TGA analysis of (black-line) ATA-SPIO and (red-line) TA-SPIO.

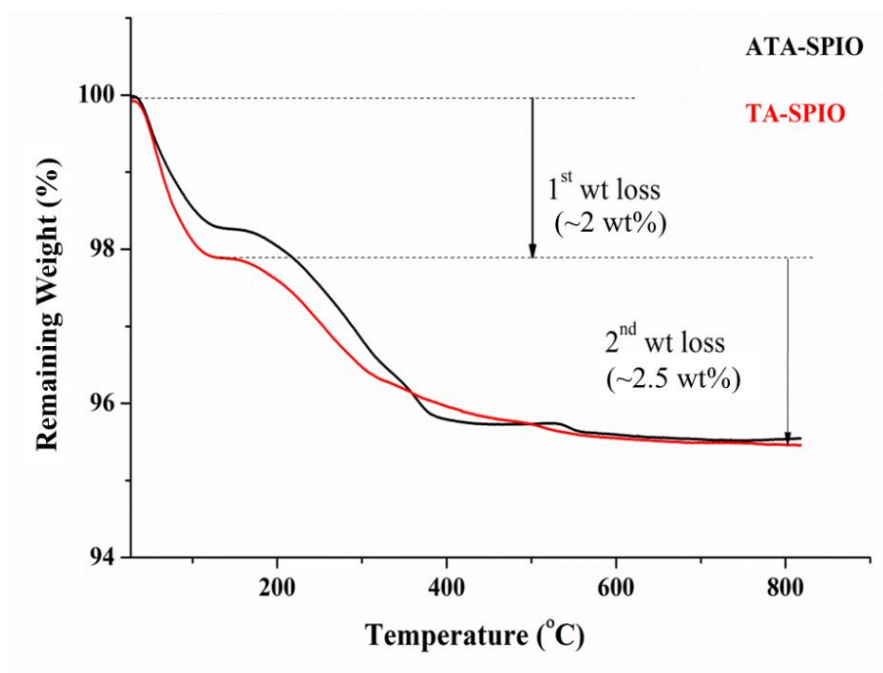


Figure S7: DLS measurements of ATA-SPIO ferrofluid suspension in DI water (pH = 7) after 24 h of storage in dark at room temperature. The concentration of ATA-SPIO nanoparticles was ~39 ppm, which corresponds to [Fe] ~ 0.50 mM. The mean hydrodynamic size was ~146 nm (100 % Number).

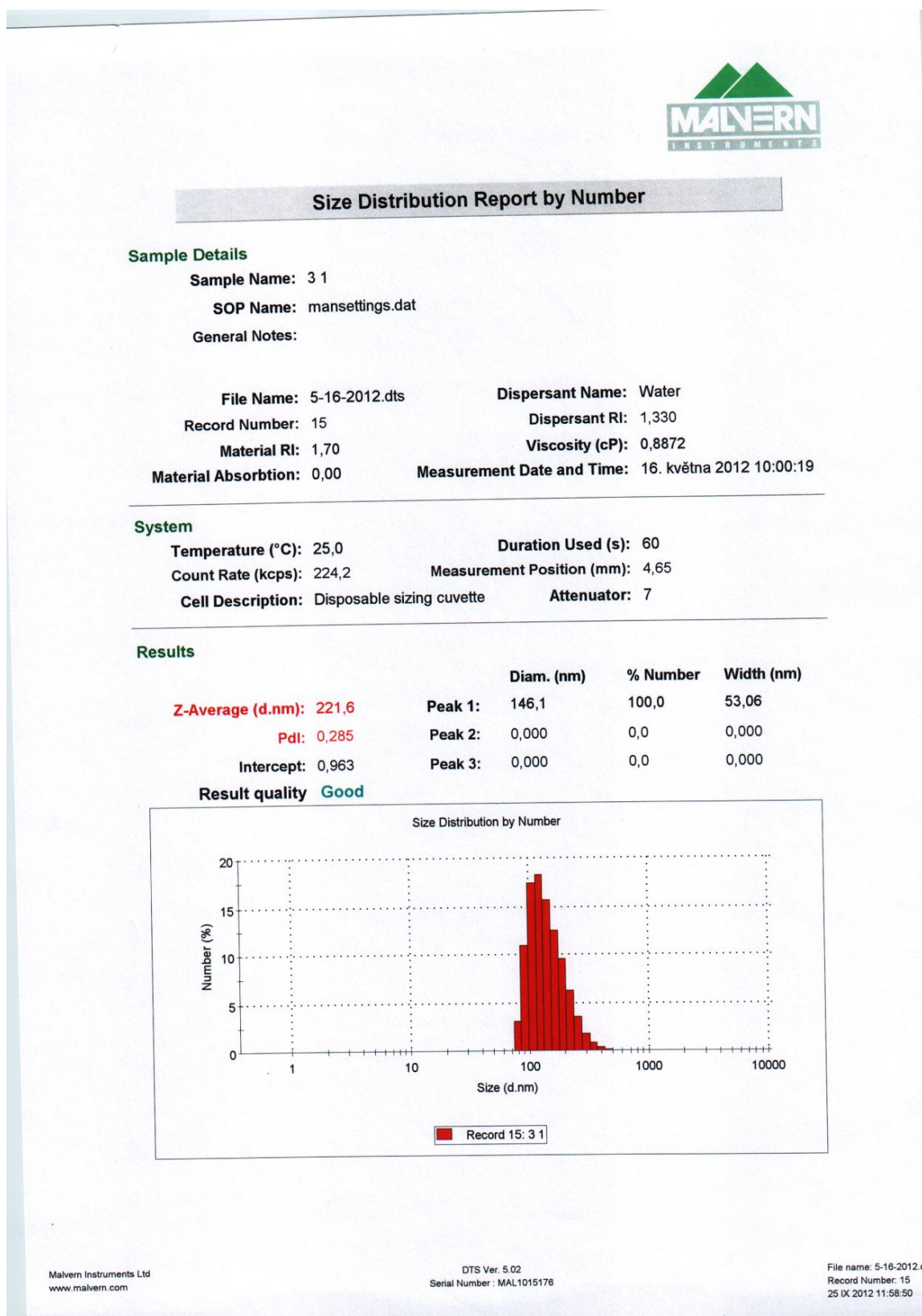


Figure S8: The zeta-potential for ATA-SPIO ferrofluid suspension in DI water (pH = 7) after 24 h of storage in dark at room temperature. The concentration of ATA-SPIO nanoparticles was ~39 ppm, which corresponds to [Fe] ~ 0.50 mM.

Zeta Potential Report

v2.2



Malvern Instruments Ltd - © Copyright 2008

Sample Details

Sample Name: 1a 3
SOP Name: mansettings.dat
General Notes:

File Name: 5-16-2012.dts Dispersant Name: Water
Record Number: 4 Dispersant RI: 1.330
Date and Time: Wednesday, May 16, 2012 9:04:3... Viscosity (cP): 0.8872
Dispersant Dielectric Constant: 78.5

System

Temperature (°C): 24.9 Zeta Runs: 102
Count Rate (kcps): 177.8 Measurement Position (mm): 2.00
Cell Description: Clear disposable zeta cell Attenuator: 7

Results

	Mean (mV)	Area (%)	Width (mV)
Zeta Potential (mV): 9.26	Peak 1: 9.26	100.0	5.47
Zeta Deviation (mV): 5.47	Peak 2: 0.00	0.0	0.00
Conductivity (mS/cm): 0.00382	Peak 3: 0.00	0.0	0.00

Result quality : **Good**

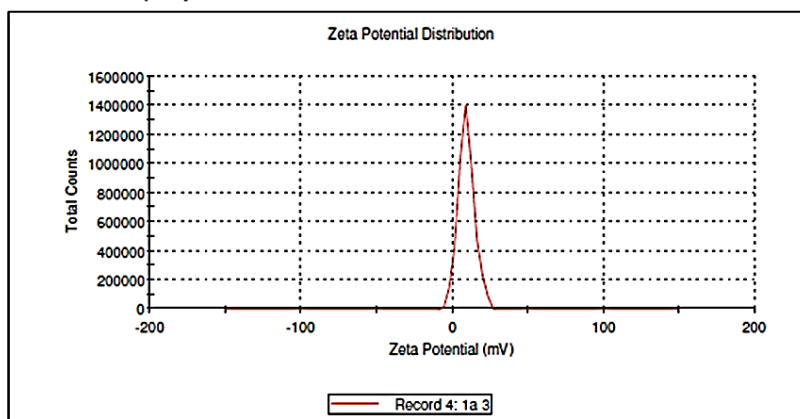


Figure S9: DLS measurements of ATA-SPIO ferrofluid suspension in DI water (pH = 7) after being aged for more than 3 months in dark at 4 °C. The concentration of ATA-SPIO nanoparticles was ~39 ppm, which corresponds to [Fe] ~ 0.50 mM.

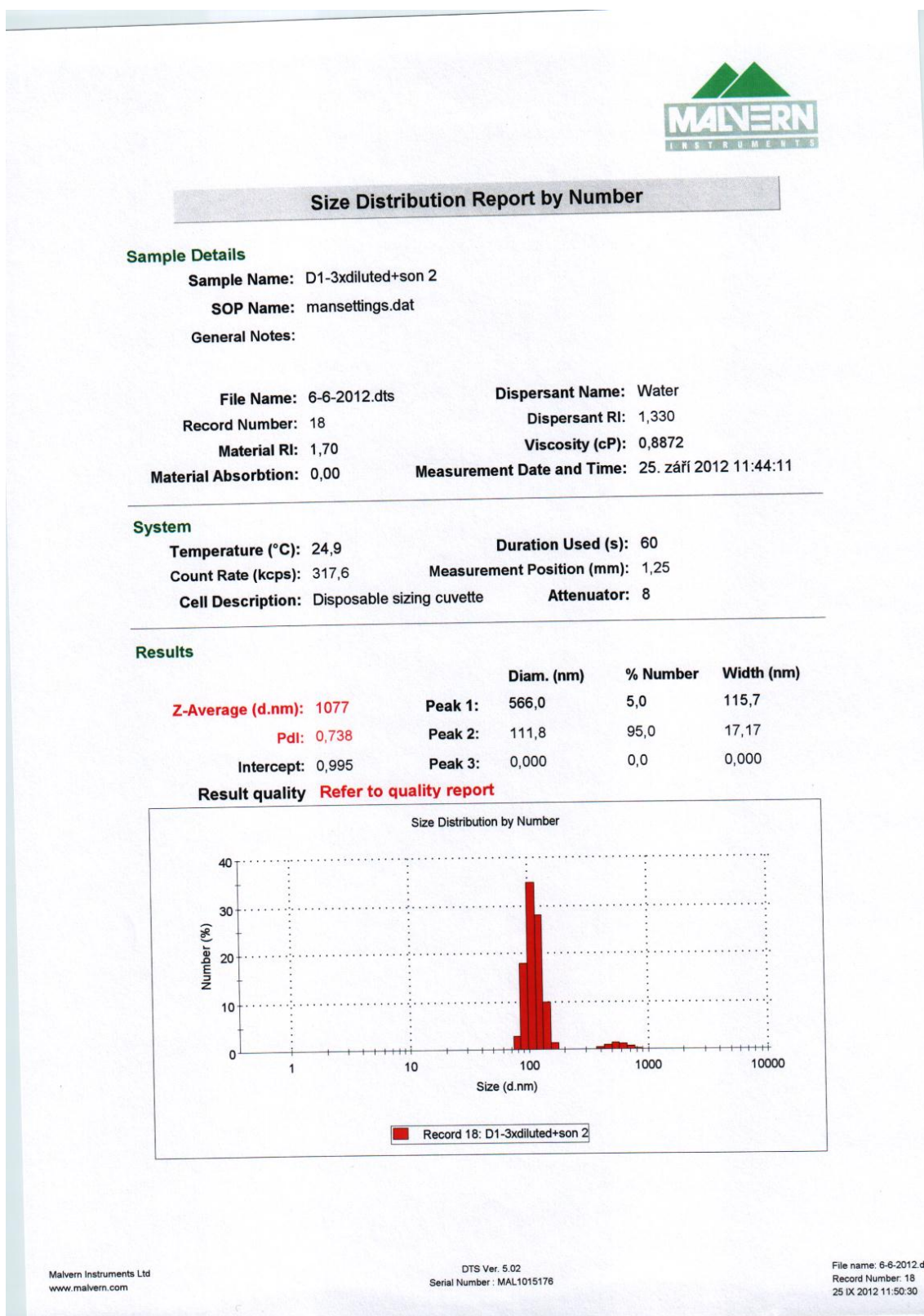


Figure S10: DLS measurements of TA-SPIO ferrofluid suspension in DI water (pH = 7) after 24 h of storage in dark at room temperature. The concentration of TA-SPIO nanoparticles was 38 ppm, which corresponds to [Fe] ~ 0.48 mM. The mean hydrodynamic size was ~124 nm (100 % Number).

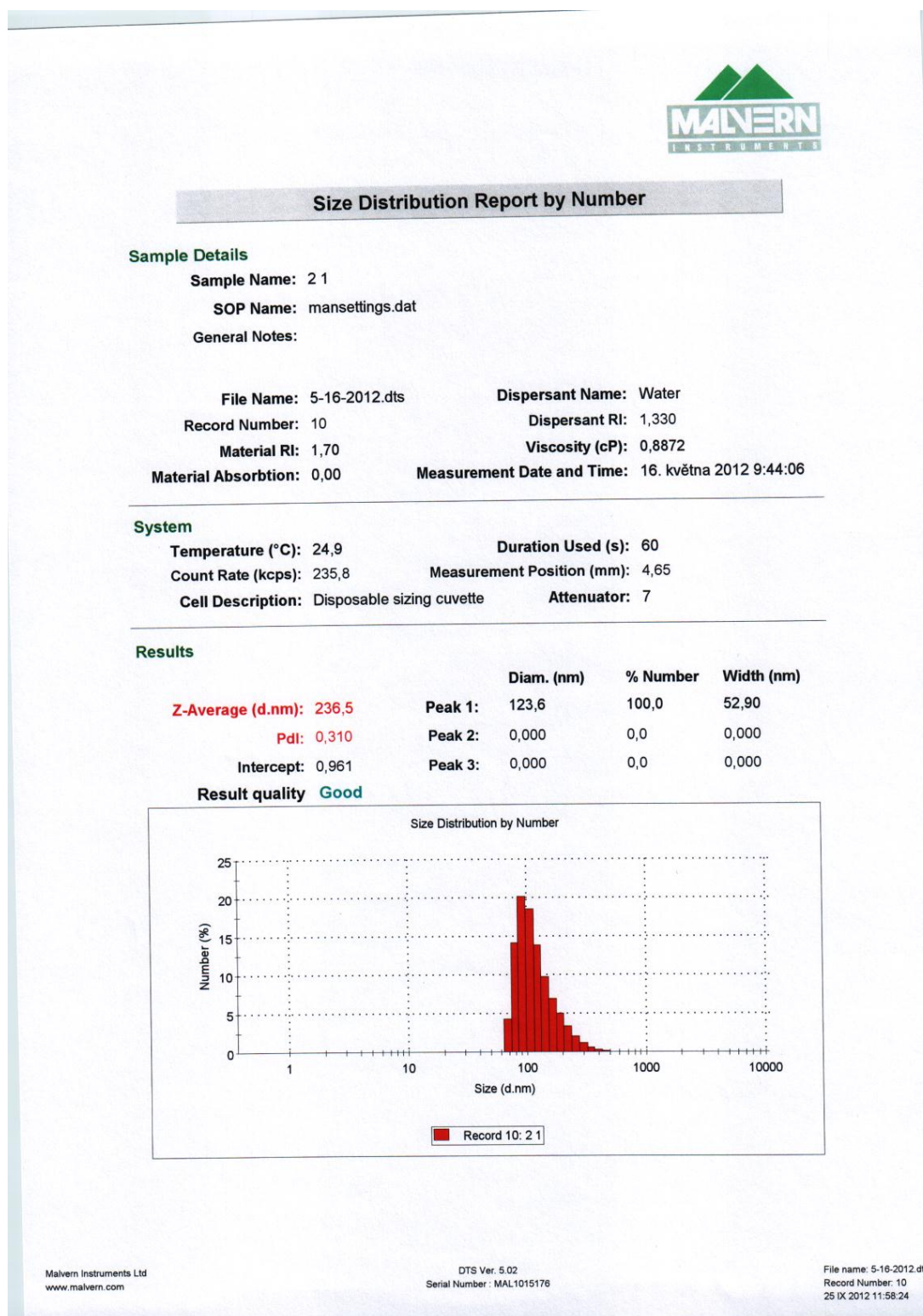


Figure S11: The zeta-potential of the TA-SPIO ferrofluid suspension in DI water (pH = 7) after 24 h of storage in dark at room temperature. The concentration of TA-SPIO nanoparticles was 38 ppm, which corresponds to [Fe] ~ 0.48 mM.

Zeta Potential Report v2.2



Malvern Instruments Ltd. © Copyright 2008

Sample Details

Sample Name: 2 1

SOP Name: mansettings.dat

General Notes:

File Name: 5-16-2012.dts	Dispersant Name: Water
Record Number: 8	Dispersant RI: 1.330
Date and Time: Wednesday, May 16, 2012 9:31:3...	Viscosity (cP): 0.8872
	Dispersant Dielectric Constant: 78.5

System

Temperature (°C): 25.0	Zeta Runs: 12
Count Rate (kcps): 125.0	Measurement Position (mm): 2.00
Cell Description: Clear disposable zeta cell	Attenuator: 7

Results

	Mean (mV)	Area (%)	Width (mV)
Zeta Potential (mV): 17.5	Peak 1: 17.5	100.0	5.78
Zeta Deviation (mV): 5.78	Peak 2: 0.00	0.0	0.00
Conductivity (mS/cm): 0.00262	Peak 3: 0.00	0.0	0.00

Result quality : **Good**

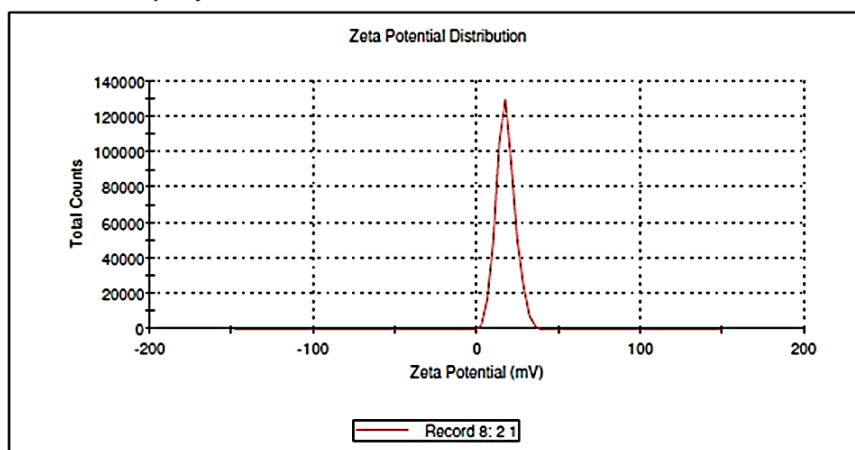


Figure S12: DLS measurements of the TA-SPIO ferrofluid suspension in DI water (pH = 7) after being aged for more than 3 months in dark at 4 °C. The concentration of ATA-SPIO nanoparticles was ~39 ppm, which corresponds to [Fe] ~ 0.48 mM.

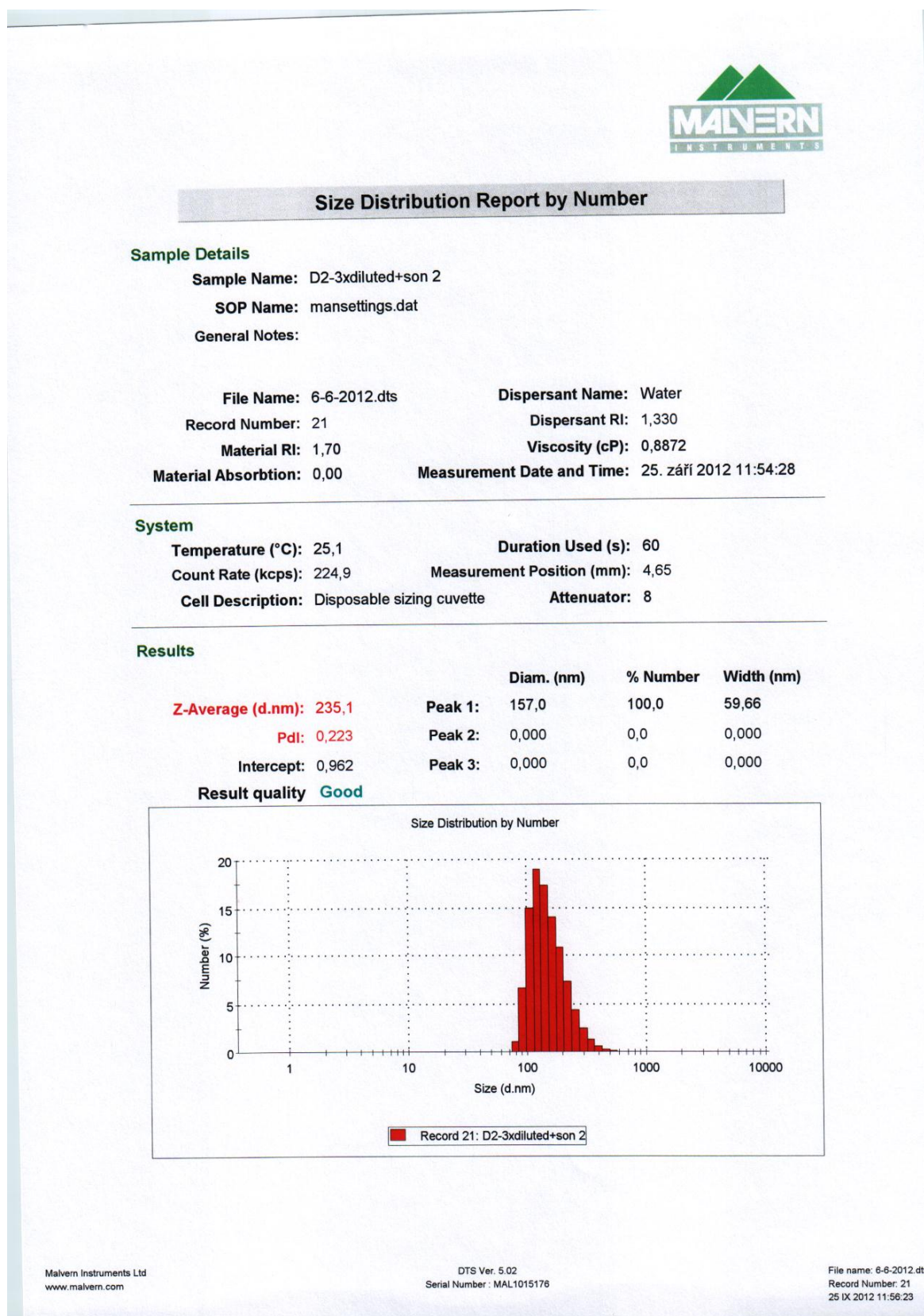


Figure S13: DLS measurements of the ATA-SPIO ferrofluid suspension in physiological salt solution (pH = 7, 150 mM of NaCl final concentration) after 1 day of storage in dark at room temperature. The concentration of ATA-SPIO nanoparticles was ~39 ppm, which corresponds to [Fe] ~ 0.50 mM. The mean hydrodynamic size was ~164 nm (100 % Number). See **Figure S7** for comparison without NaCl.

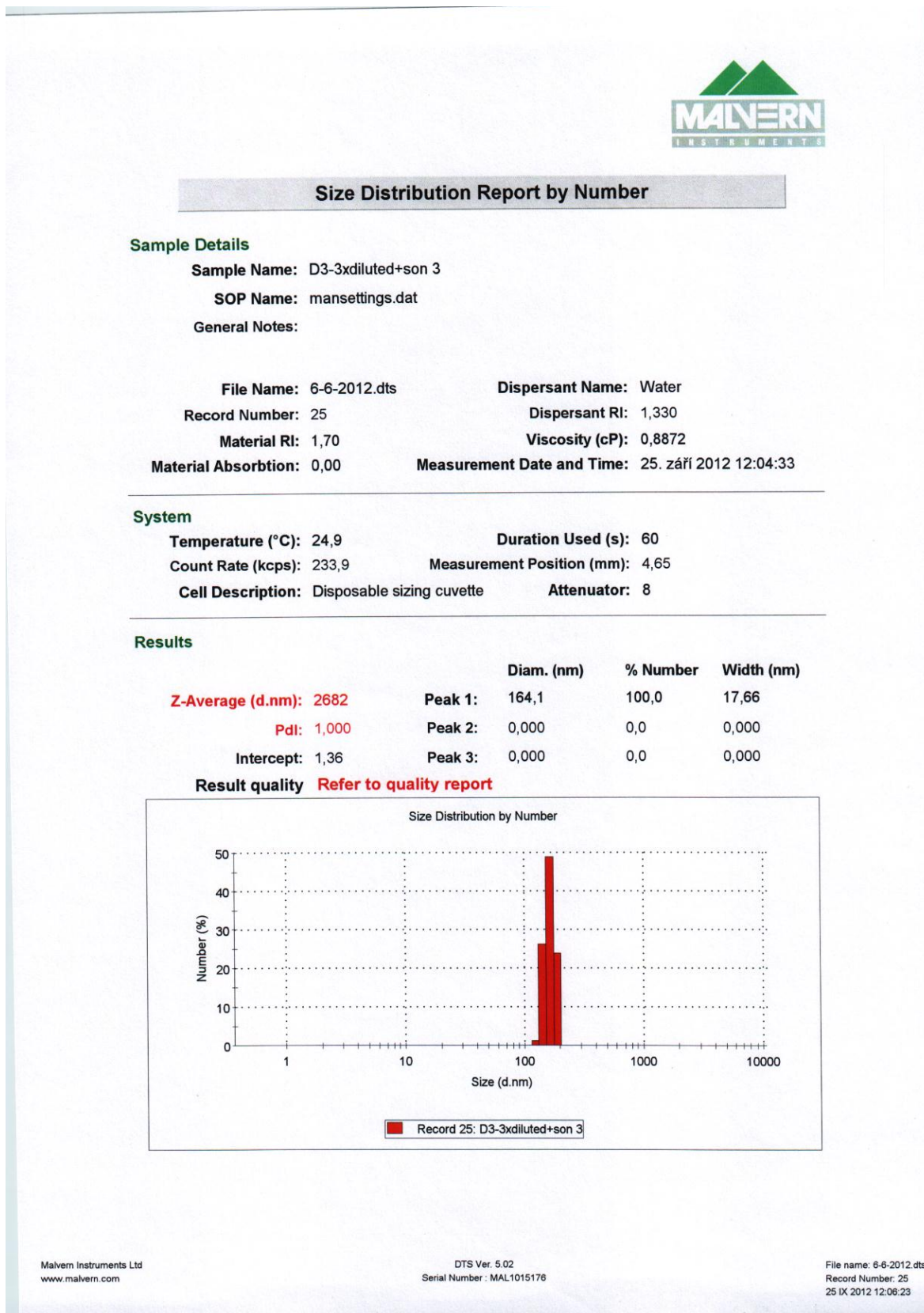


Figure S14: DLS measurements of the ATA-SPIO ferrofluid suspension in physiological salt solution (pH = 7, 150 mM of NaCl final concentration) after 1 day of storage in dark at room temperature. The concentration of ATA-SPIO nanoparticles was 38 ppm, which corresponds to [Fe] ~ 0.48 mM. The mean hydrodynamic size was ~408 nm (100 % Number). See **Figure S10** for comparison without NaCl.

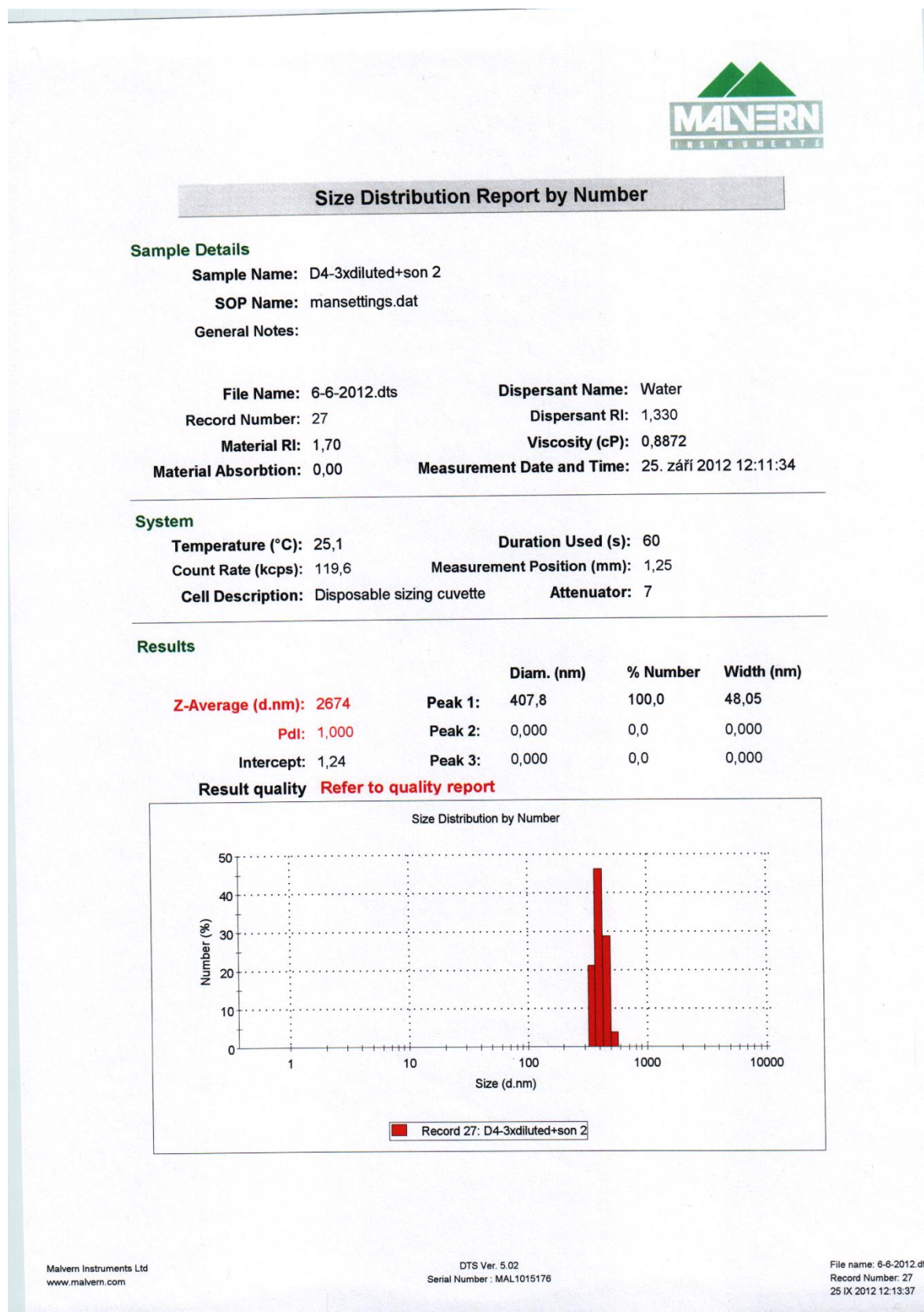


Figure S15: Plots for r_1 , r_2 and r_2^* of ATA-SPIO nanoparticles.

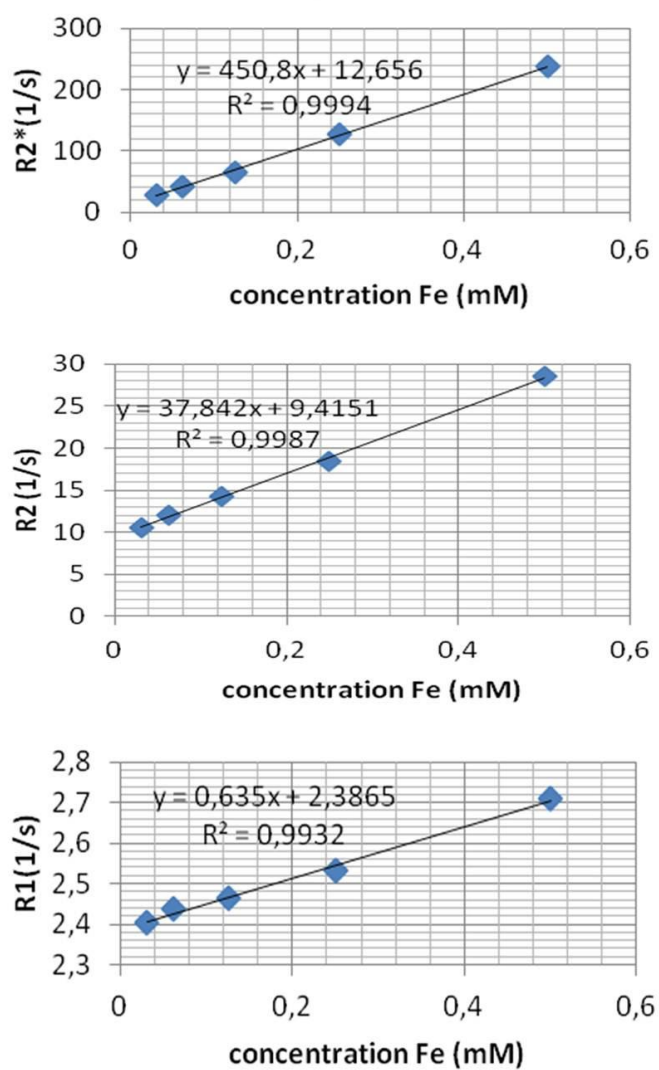


Figure S16: Plots for r_1 , r_2 and r_2^* of TA-SPIO nanoparticles.

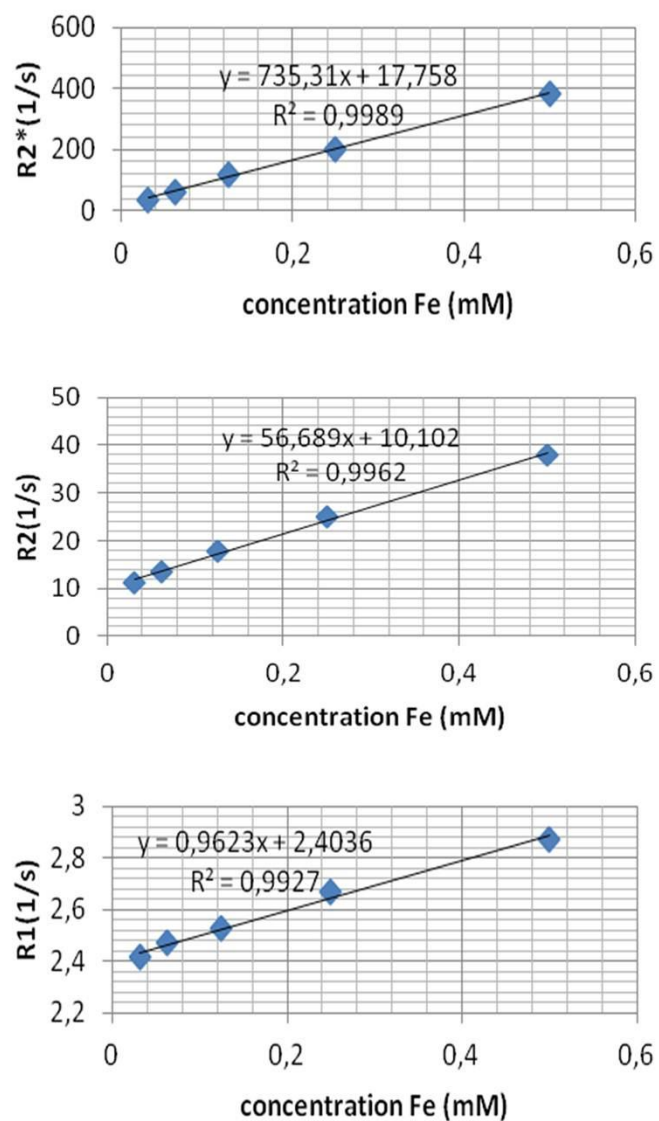


Figure S17: Negative of the phantom experiment acquired under T_2^* weighted image, left TA-SPIO and right ATA-SPIO with concentrations (mM) reported below each spot.

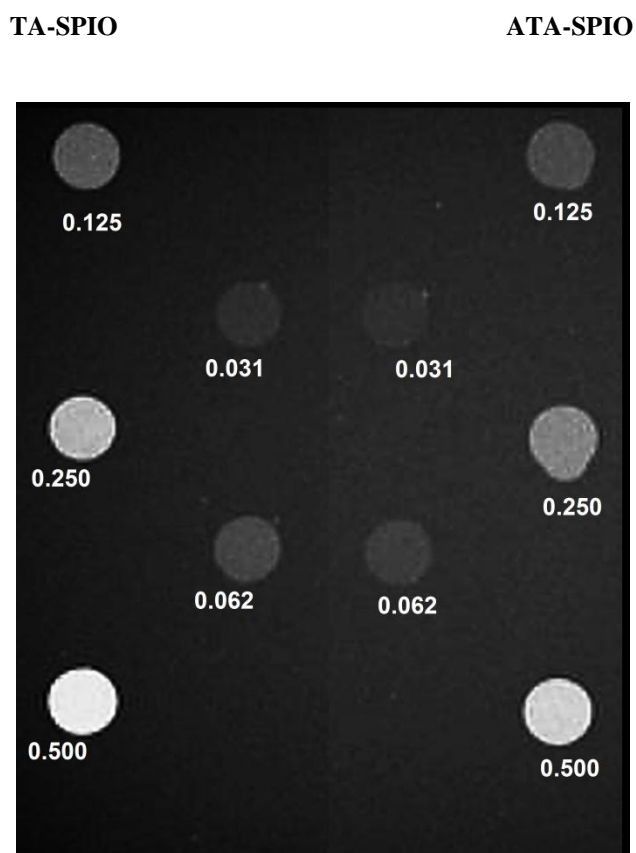
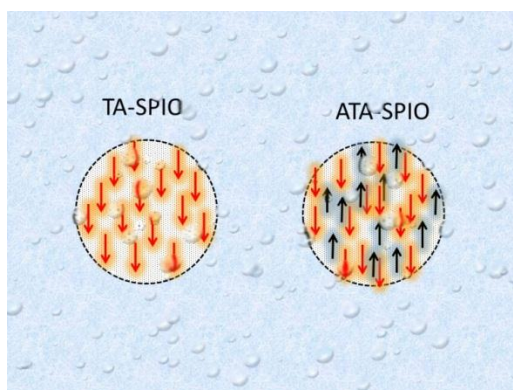
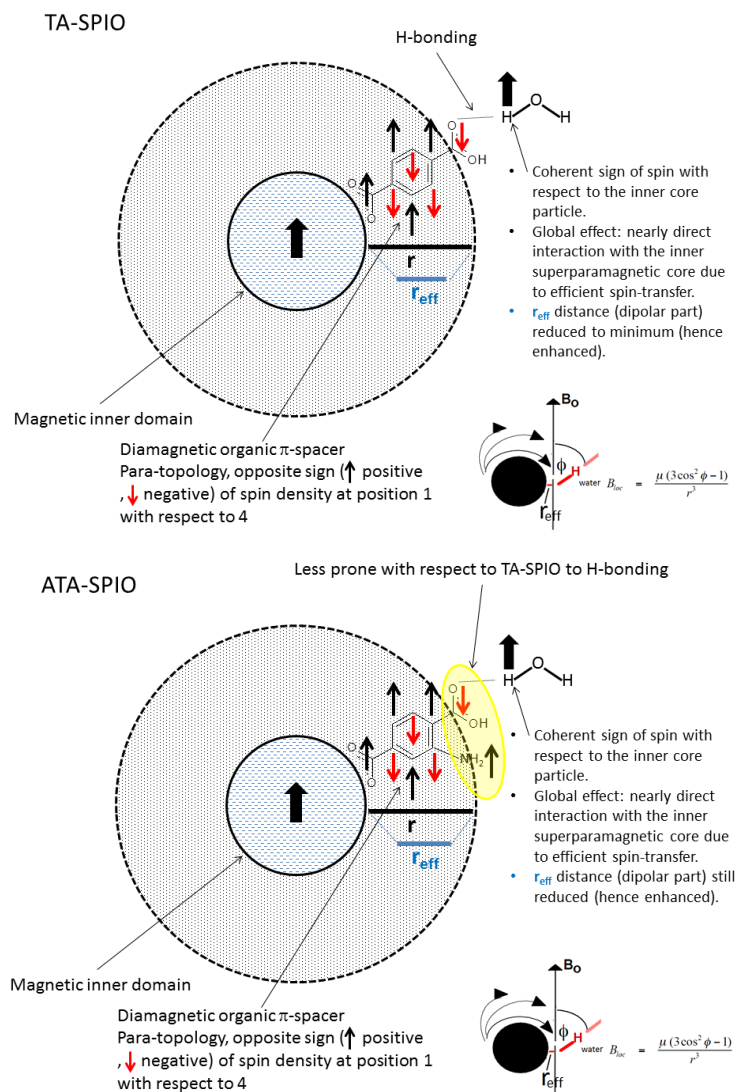


Figure S18. The diverse interactions between nanoparticle (SPIO NP) and water molecule due to the minor differences in chemical identity of the organic coatings: (**top figure**) in TA-SPIO, H-bonding interaction with surrounding water is very efficient, in ATA-SPIO (**middle figure**) intramolecular H-bonding interaction, between carboxylate and ortho amino-group, may act as competing process with the H-bonding with surrounding water. In addition, opposite signs for the spin-polarization are present at -COOH and -NH₂ moieties. The **lowest figure** shows surface renderings: in ATA-SPIO areas with opposite signs (positive ↑ and negative ↓) of the spin density should be present at the SPIO NP surface, differing from TA-SPIO (homogeneous sign). The figures depicted serve as cartoons for easier visualization of our hypothesis for the active physical processes underneath the MRI results.



Supporting Tables S1-S3

Table S1: Parameters of the M-H curves measured at 5 K and 300 K, where $M_{\max+}$ (7 T) and $M_{\max-}$ (-7 T) are the maximum magnetization at 7 T and -7 T, H_{C+} and H_{C-} are the positive and negative coercivity, M_{R+} and M_{R-} are the positive and negative remnant magnetization, respectively.

Sample	<i>T</i> (K)	$M_{\max+}$ (7 T) ± 0.01 (emu/g)	$M_{\max-}$ (-7 T) ± 0.01 (emu/g)	H_{C+} ± 5 (Oe)	H_{C-} ± 5 (Oe)	M_{R+} ± 0.01 (emu/g)	M_{R-} ± 0.01 (emu/g)
ATA -SPIO	5	83.99	- 83.99	189	- 197	19.90	- 19.79
	300	73.60	- 73.60	18	- 18	2.18	- 2.25
TA-SPIO	5	83.27	- 83.27	268	- 278	23.19	- 22.38
	300	74.32	- 74.32	14	- 14	1.62	- 1.62

Table S2: Mössbauer hyperfine parameters derived from the Mössbauer spectra of the TA-SPIO (**Panel a**) and ATA-SPIO (**Panel b**) samples, measured at $T = 150$ K, where δ is the isomer shift, ΔE_Q is the quadrupole splitting, B_{hf} is the hyperfine magnetic field, and RA is the relative spectral area of the individual spectral components. *Since the sextet spectral component was fitted with a distribution of the magnetic hyperfine fields, the value of B_{hf} corresponds to the most probable value derived from the particular profile of the B_{hf} -distribution.

Sample	T (K)	Component	$\delta \pm 0.01$ (mm/s)	$\Delta E_Q \pm 0.01$ (mm/s)	$B_{\text{hf}} \pm 0.3$ (T)	RA ± 1 (%)	Assignment
(Panel b) ATA-SPIO	150	Sextet 1	0.38	0.00	48.9	57	Tetrahedral and octahedral Fe ³⁺
		Sextet 2	0.57	0.00	44.5	43	Octahedral Fe ²⁺ -Fe ³⁺
(Panel a) TA-SPIO	150	Sextet 1	0.39	0.00	48.4	58	Tetrahedral and octahedral Fe ³⁺
		Sextet 2	0.55	0.00	43.8	42	Octahedral Fe ²⁺ -Fe ³⁺

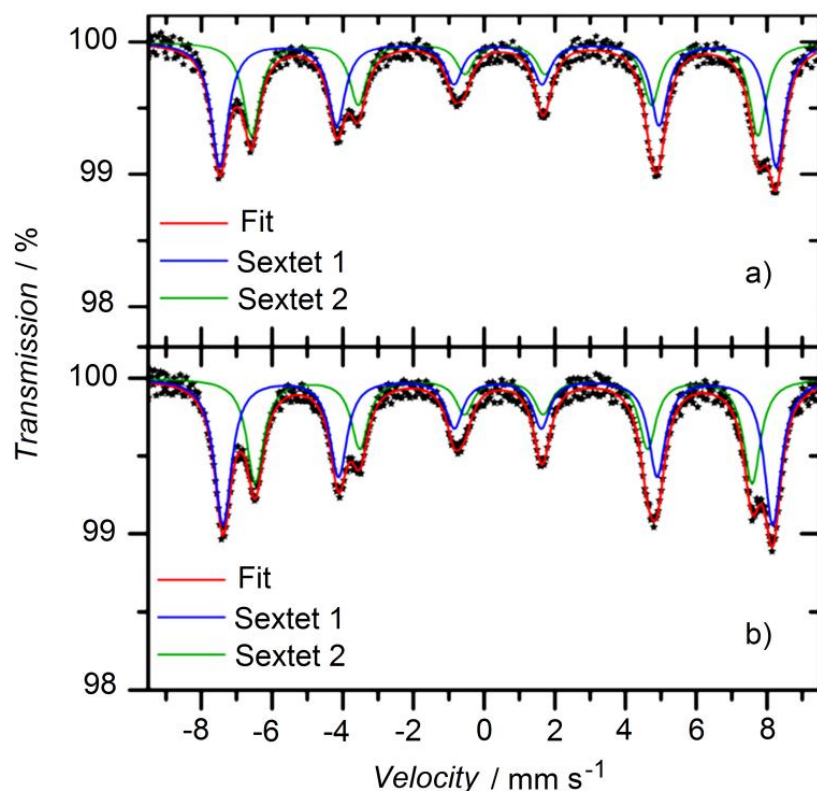


Table S3: Relaxivity indexes r_1 , r_2 and r_2^* of ATA-SPIO and TA-SPIO nanoparticles.

Samples	Relaxivity ($\text{mM}^{-1}\text{s}^{-1}$)		
	r_1	r_2	r_2^*
ATA-SPIO	0.635	37.8	450.8
TA-SPIO	0.962	56.7	735.3